A Comprehensive Evaluation of CUSUM Control Chart Performance for a SARFIMAX Model with Exponential White Noise

WILASINEE PEERAJIT
Department of Applied Statistics, Faculty of Applied Science,
King Mongkut's University of Technology North Bangkok,
Bangkok 10800,
THAILAND

Abstract: - The cumulative sum (CUSUM) control chart is widely recognized for its superior ability to detect small to moderate upward shifts in the process mean. This study focuses on accurately approximating the average run length (ARL) of a CUSUM chart applied to a long-memory SARFIMAX(p, d, q, x)×(P, D, Q)$_s$ model with exponential white noise. The model accommodates both seasonality and fractional differencing, providing flexibility for complex time-series structures. ARL values are approximated through numerical integral equations (NIEs) using Gaussian quadrature, midpoint, trapezoidal, and Simpson's rules. Comparative results indicate that all four approaches yield highly consistent ARL estimates, confirming the robustness of the NIE framework. Among them, the midpoint rule demonstrates the lowest computational time while maintaining high accuracy, as reflected by its minimal percentage relative deviation (%Dev). These findings highlight the computational efficiency and sensitivity of the proposed method, supporting its practical applicability in real-world process monitoring scenarios.

Key-Words: - Average run length (ARL), SAFIMAX(p, d, q, x)×(P, D, Q)$_s$, exponential white noise, numerical integral equation (NIE) method, midpoint rule, trapezoidal rule, Gaussian rule, Simpson's rule.

Received: March 27, 2026. Revised: May 11, 2026. Accepted: May 25, 2026. Published: July 27, 2026.

1 Introduction

The primary purpose of a control chart is to promptly trigger an out-of-control signal when the process exhibits instability. The change may affect the process mean and/or dispersion, which are often regulated process parameters. In the field of statistical process control, the most commonly applied control charts for monitoring process parameters are the Shewhart, cumulative sum (CUSUM), and exponentially weighted moving-average (EWMA) control charts, [1]. Control charts are classified as either memoryless or memory-type depending on whether historical data are involved. The Shewhart control chart is memoryless as it solely depends on current data. It is adept at identifying significant shifts in a process parameter but exhibits reduced sensitivity to minor or moderate variations. In contrast, the CUSUM and EWMA control charts are the memory-type, [2], [3], employing both current and historic data to rapidly detect small and moderate shifts. They are extensively used in the processing and service industries due to their ability to detect minor or moderate changes.

The CUSUM control chart has been employed in various fields, including manufacturing (e.g., precision machining, electronics), healthcare (e.g., monitoring surgical outcomes), pharmaceuticals (e.g., ensuring drug quality), and finance (e.g., identifying shifts in time-series data), [4]. Consequently, we adopted the CUSUM control chart to evaluate process parameter shifts and monitor performance.

One of the key metrics used to assess the performance of a control chart is the average run length (ARL). It represents the expected number of observations taken before a control chart signals a change in a process parameter. There are two primary components of the ARL. The in-control ARL (ARL_0) represents when the process is operating stably, with the value set sufficiently high to avoid false alarms. For the CUSUM control chart, this is configured by modifying the threshold parameter. Conversely, the out-of-control ARL (ARL_1) represents when the process parameter deviates from the standard value. In conclusion, a highly sensitive chart is configured using a sufficiently large ARL_0 to reduce false alarms (e.g., 370) and the smallest ARL_1 possible to detect changes in the process parameter signaling that the process is out of control.

To determine the ARL for a process on the CUSUM control chart, it is usually assumed that the observations are independent and identically distributed (i.i.d.) and follow a normal distribution. However, in practice, process data may display autocorrelation or conform to time-series models, such as autoregressive (AR), moving-average (MA), ARMA, AR integrated MA (ARIMA), or AR fractionally integrated MA (ARFIMA).

The establishment of stochastic analysis of a time series is credited to the pioneering work of [5], [6], who developed AR and MA models. In the study, [7], provided a systematic inferential analysis of stationary ARMA models, which became essential for applied time-series research. The introduction of long-memory processes by [8], [9], marked the beginning of a promising research trajectory for time-series analysts and econometricians. ARFIMA processes, in which a fractional amount of differencing is employed, are now used in many areas such as energy pricing and demand, telecommunications, environmental time series, and financial volatility, [10], [11], [12].

Using the ARL for CUSUM control chart performance evaluation is relevant in these cases, although the formula to calculate it is more complex. Researchers have examined the performance of the CUSUM control chart with autocorrelated data and developed ARL formulas for various time-series models, such as AR(1), [13], ARIMA(p, d, q), [14], and ARFIMA(p, d, q), [15], among others. In the present study, we examined seasonal ARFIMA (SARFIMA) models useful for analyzing seasonal time series where the mean and other statistical measures are not stationary over time. The SARFIMA model is a straightforward extension of the ARFIMA model previously discussed. Recently, SARFIMA models have been applied to analyze various real-world cyclical phenomena that display long-range dependence. For instance, river flows, [16], money supply, [17], income trends over time, [18], inflation rates, [19], quarterly gross national product, and shipping data, [20].

Exogenous variables can be incorporated into ARFIMA models (i.e., ARFIMAX) to enhance their performance. The study, [21], was the first to present the ARFIMAX model and applied it to estimate the realized volatilities within a Dow Jones Industrial Average portfolio. Conversely, in 2008, [22], focused on estimating and forecasting daily price changes using both ARFIMAX and ARFIMAX-threshold autoregressive conditional heteroskedasticity (TARCH) models.

For modeling seasonal time series, white noise is typically characterized by a Gaussian distribution. However, in various applications, the noise can be exponentially distributed, which has been utilized in numerous research studies, [23], [24], [25], [26].

Many numerical integration equations (NIE) methods based on the Gaussian quadrature, midpoint, trapezoidal, and Simpson's rules have been proposed to compute or approximate the ARL for processes on a CUSUM control chart. These methods offer practical solutions for approximating the ARL, particularly when analytical expressions are intractable, and have been widely used in studies involving both short- and long-memory processes, as well as non-Gaussian white noise. In the study, [27], presented explicit expressions for the ARL on a lower-sided negative CUSUM control chart while assuming that the observations follow an exponential distribution. The authors compared the accuracy and efficiency of these expressions against ARL approximations obtained through the midpoint rule-based NIE approach. Building on this, [28], approximated the ARL for the CUSUM control chart with an SARX$(P,1)_S$ process with exponential white noise. They employed four NIE based on the midpoint, trapezoidal, Simpson's, and Gauss-Legendre quadrature rules and evaluated each in terms of computational efficiency and accuracy. Further expanding the scope, [29], applied the Gauss-Legendre quadrature rule-based NIE approach to approximate the ARL for a fractionally integrated ARX model. This work marked a significant extension of the NIE approach to more complex time series structures.

Herein, we propose NIE approaches based on the Gaussian quadrature, midpoint, trapezoidal, and Simpson's rules to approximate the ARL of a SAFIMAX$(p, d, q)\times(P, D, Q)_s$ model characterized by exponential white noise and long-memory behavior on a CUSUM control chart. Furthermore, a numerical comparison of the ARL results from each method was conducted, with a particular focus on their computational efficiency.

2 Methodology

2.1 Description of one-sided CUSUM control chart

The focus of this study is on the upper-sided CUSUM control chart using a single CUSUM statistic $(C_t,\ t=1,2,...,)$ to detect small-to-moderate upward shifts in the mean of a SARFIMAX process defined as

$$C_t = \max\{0,\ C_{t-1} + Y_t - K\}, \tag{1}$$

where K represents the reference parameter, Y_t is a generalization of a long-memory SAFIMAX(p, d, q, x) $\times$(P, D, Q)$_s$ process. Here, the initial value of the CUSUM control chart statistic is $C_0 = \varphi$, where $0 \le \varphi \le b$.

The stopping time (τ_b) for the alarm signal of the upper-sided CUSUM control chart is defined as

$$\tau_b = \inf\{t > 0;\ C_t > b\}, \tag{2}$$

where b is the upper control limit (UCL) of the CUSUM control chart.

In this work, the value of K can be 2.5, 2.75, or 3.0 based on the decision interval for b, to achieve a target ARL$_0$ value of 100, 370, or 500, respectively.

2.2 Description of SARFIMAX Time Series

The SARFIMA model is defined by the notation SAFIMAX(p, d, q, x)$\times$(P, D, Q)$_s$, where p and P represent the orders of the non-seasonal AR and seasonal AR (SAR) terms, and q and Q denote the orders of the non-seasonal MA and seasonal MA (SMA) terms, and d and D represent the degrees of non-seasonal and seasonal differencing, respectively. For long-memory time series, the SARFIMA model's performance can be significantly enhanced through the inclusion of exogenous variables to provide the SARFIMAX model, [22].

Definition 1: Let $Y_t,\ t=1,2,...,$ be the sequence of a SAFIMAX(p, d, q, x)$\times$(P, D, Q)$_s$ process with underlying white noise defined as follows:

$$\phi(B)\Phi(B^S)\nabla^d\nabla_S^D Y_t = \theta(B)\Theta(B^S)\varepsilon_t + \sum_{i=1}^{n}(\omega_i X_{it}), \tag{3}$$

where $X_{it},\ i=1,2,...,$ the exogenous variables $\omega_i,\ i=1,2,...,$ are unknown parameters, and $\varepsilon_t,\ t=1,2,...,$ is a sequence of continuous i.i.d. random variables from an exponential distribution with mean α, that are mean-centered (i.e., $E(\varepsilon_t)=1/\alpha$, so the in-control mean is α_0). In addition, $\phi(B)$, $\Phi(B^S)$, $\theta(B)$, and $\Theta(B^S)$ are finite AR, SAR, MA, SMA polynomials of order $p, q, P,$ and Q, respectively, defined as

$$\phi_p(B) = 1 - \phi_1 B - \phi_2 B^2 - ... - \phi_p B^p,$$
$$\theta_q(B) = 1 - \theta_1 B - \theta_2 B^2 - ... - \theta_q B^q,$$
$$\Phi_P(B^S) = 1 - \Phi_1 B^s - \Phi_2 B^{2s} - ... - \Phi_P B^{PS}, \text{ and}$$
$$\Theta_Q(B^S) = 1 - \Theta_1 B^S - \Theta_2 B^{2S} - ... - \Theta_Q B^{QS},$$

where S represents the seasonal period (12 in the case of monthly data) and B is a backward-shift operator used to define lagged observations ($BY_t = Y_{t-1}$, and $B^s Y_t = Y_{t-s}$.).

Definition 2: The non-seasonal $\nabla^d := (1-B)^d$ and seasonal $\nabla_S^D := (1-B^S)^D$ fractional differencing operators allow differencing a time series to non-integer degrees d and D, respectively. These operators are respectively denoted as

$$(1-B^S)^D = \sum_{k=0}^{\infty}\binom{D}{k}(-B^S)^k. \tag{4}$$

where $\binom{D}{k} = \frac{\Gamma(D+1)}{\Gamma(k+1)\Gamma(D-k+1)}$, $\Gamma(.)$ is a gamma function, and $S=1$ and $D=d$ (i.e., $\nabla_S^D = \nabla^d$.).

Definition 3: The inverse fractional differencing operators for non-seasonal and seasonal fractional differencing operators are defined as

$$(1-B^S)^{-D} = \sum_{k=0}^{\infty}\binom{D+k-1}{k}(B^S)^k. \tag{5}$$

where $\binom{D+k-1}{k} = \frac{\Gamma(D+k)}{\Gamma(D)\Gamma(k+1)}$, $B^{kS}Y_t = Y_{t-kS}$ and non-seasonal fractional differencing operators $S=1$ and $D=d$.

A SAFIMAX(p, d, q, x)$\times$(P, D, Q)$_s$ time series is said to be stationary if $(d+D) < 0.5$ and $D < 0.5$, and exhibits long-memory when $0 < (d+D) < 0.5$ and $0 < D < 0.5$. Conversely, it displays intermediate memory if $-0.5 < (d+D) < 0$, and $-0.5 < D < 0$. The series becomes nonstationary when $D > 0.5$. Finally, if $d=0$ and $D=0$, the model simplifies to a seasonal ARMA model.

Based on Definitions 1 and 3, the long-memory SAFIMAX(p, d, q, x)$\times$(P, D, Q)$_s$ process with exponential white noise on the CUSUM control chart can be written as

$$Y_t = (1-\phi_1 B - ... - \phi_p B^p)^{-1}(1-\Phi_1 B^s - ... - \Phi_P B^{PS})^{-1}(1-B)^{-d}$$
$$(1-B^S)^{-D}(1-\theta_1 B - ... - \theta_q B^q)(1-\Theta_1 B^S ... - \Theta_Q B^{QS}) + \sum_{i=1}^{n}(\omega_i X_{it}).$$

or

$$Y_t = (1-\sum_{i=1}^{p}\phi_i B^i)^{-1}(1-\sum_{k=1}^{P}\Phi_k B^{ks})^{-1}(1-B)^{-d}(1-B^S)^{-D}$$
$$(1-\sum_{j=1}^{q}\theta_j B^j)(1-\sum_{l=1}^{Q}\Theta_l B^{ls})\varepsilon_t + \sum_{i=1}^{n}(\omega_i X_{it}). \qquad (6)$$

The SAFIMAX(p, d, q, x)×(P, D, Q)$_s$ model specifications used in the simulation study are as follows:

1) Long-memory SAFIMAX(1, 0.1, 1, 1)×(1, 0.2, 1)$_{12}$ model is
$$(1-0.1B)(1-0.1B^{12})(1-B)^{0.1}(1-B^{12})^{0.2}Y_t = (1-0.1B)(1-0.1B^{12})\varepsilon_t + 0.3X_{1t}$$
2) Long-memory SAFIMAX(1, 0.1, 1, 1)×(1, 0.2, 2)$_{12}$ model is
$$(1-0.1B)(1-0.1B^{12})(1-B)^{0.1}(1-B^{12})^{0.2}Y_t = (1-0.1B)(1-0.1B^{12}-0.2B^{24})\varepsilon_t + 0.3X_{1t}$$

3 Approximating the ARL of a SARFIMAX model on a CUSUM control chart via the NIE-based approaches

The ARL of SAFIMAX(p, d, q, x)×(P, D, Q)$_s$ time-series models on a CUSUM control chart can be approximated using four NIE approaches based on the Gaussian quadrature, midpoint, trapezoidal, and Simpson's rules.

Let $\mathrm{L}(\varphi) = E_\infty(\tau_b) < \infty$ represent the ARL of the upper-sided CUSUM control chart corresponding to the initial value (φ) for a SAFIMAX(p, d, q, x)×(P, D, Q)$_s$ model with exponential white noise. The lower control limit (LCL) and upper control limit (UCL) are denoted as 0 and b, respectively.

For a process that is in control, the CUSUM statistic satisfies the condition $0 \le C_t \le b.$, with a value of C_t exceeding b indicating the out-of-control condition. Function $\mathrm{L}(\varphi)$ derived using the Fredholm integral equation of the second kind, [30], can be expressed as

$$\mathrm{L}(\varphi) = 1 + \int_0^b \mathrm{L}(z)\, f\Bigg(z + K - \varphi - (1-\sum_{i=1}^{p}\phi_i B^i)^{-1}(1-\sum_{k=1}^{P}\Phi_k B^{ks})^{-1}$$
$$.(1-B)^{-d}(1-B^S)^{-D}(1-\sum_{j=1}^{q}\theta_j B^j)(1-\sum_{l=1}^{Q}\Theta_l B^{ls})\varepsilon_t + \sum_{i=1}^{n}(\omega_i X_{it})\Bigg)dz$$
$$+ \mathrm{L}(0)F\Bigg(K - \varphi - (1-\sum_{i=1}^{p}\phi_i B^i)^{-1}(1-\sum_{k=1}^{P}\Phi_k B^{ks})^{-1}(1-B)^{-d}(1-B^S)^{-D}$$
$$.(1-\sum_{j=1}^{q}\theta_j B^j)(1-\sum_{l=1}^{Q}\Theta_l B^{ls})\varepsilon_t + \sum_{i=1}^{n}(\omega_i X_{it})\Bigg)dz. \qquad (7)$$

where $F(\varphi) = 1 - e^{-\alpha\varphi}$, $f(\varphi) = \alpha e^{-\alpha\varphi}$.

Consequently, the ARL result derived by using the NIE method with an initial value $C_0 = \varphi$ can be reformulated as

$$\mathrm{L}(\varphi) = 1 + \alpha e^{\alpha\left(\begin{array}{l}\varphi - K + (1-\sum_{i=1}^{p}\phi_i B^i)^{-1}(1-\sum_{k=1}^{P}\Phi_k B^{ks})^{-1}(1-B)^{-d}(1-B^S)^{-D} \\ (1-\sum_{j=1}^{q}\theta_j B^j)(1-\sum_{l=1}^{Q}\Theta_l B^{ls})\varepsilon_t + \sum_{i=1}^{n}(\omega_i X_{it})\end{array}\right)}$$
$$\int_0^b \mathrm{L}(z)e^{-\alpha z}dz + \mathrm{L}(0)\,(1 - e^{-\alpha\left(\begin{array}{l}K - \varphi - (1-\sum_{i=1}^{p}\phi_i B^i)^{-1}(1-\sum_{k=1}^{P}\Phi_k B^{ks})^{-1}(1-B)^{-d} \\ (1-B^S)^{-D}(1-\sum_{j=1}^{q}\theta_j B^j)(1-\sum_{l=1}^{Q}\Theta_l B^{ls})\varepsilon_t + \sum_{i=1}^{n}(\omega_i X_{it})\end{array}\right)}). \qquad (8)$$

This demonstrates that the quadrature rule can be applied to approximate the integral via a finite summation. The approximation of an integral across the interval [0 , b] is divided into partitions; i.e., $0 \le \upsilon_1 \le \upsilon_2 \le .... \le \upsilon_m \le b$. Thus, the approximation for the integral equation becomes

$$\int_0^b W(z)\, f(z)dz \approx \sum_{\eta=1}^{m} w_\eta f(\upsilon_\mu),\ j = 1, 2, ..., m, \qquad (9)$$

where "υ_η" represents the nodes and $W(z)$ as a *weight function*. For $W(z) = 1$, nodes, set $\{\upsilon_\eta,\ \eta = 1, 2, ..., m\}$, and set of constant weights $\{w_\eta, \eta = 1, 2, ..., m\}$ are determined by specific criteria. Function $W(z)$ is initially selected to ensure that a set of polynomials effectively approximates the function $f(\upsilon)$ that needs to be integrated. The points and weights are chosen to guarantee that the quadrature rule is exact for the highest possible degree of polynomials for $f(\upsilon)$ based on those points.

Let $\hat{\mathrm{L}}(\varphi)$ represent the NIE method for function $\mathrm{L}(\varphi)$. Equation (8) can be obtained by employing the method used for solving systems of linear algebraic equations, [30]:

$$\hat{\mathrm{L}}(\upsilon_i) = 1 + \sum_{\eta=1}^{m} w_\eta \hat{\mathrm{L}}(\upsilon_\eta)\, f\Bigg(\upsilon_j + K - \upsilon_i - (1-\sum_{i=1}^{p}\phi_i B^i)^{-1}(1-\sum_{k=1}^{P}\Phi_k B^{ks})^{-1}$$
$$.(1-B)^{-d}(1-B^s)^{-D}(1-\sum_{j=1}^{q}\theta_j B^j)(1-\sum_{l=1}^{Q}\Theta_l B^{ls})\varepsilon_t + \sum_{i=1}^{n}(\omega_i X_{it})\Bigg)$$
$$+\hat{\mathrm{L}}(\upsilon_1)F\Bigg(K - \upsilon_i - (1-\sum_{i=1}^{p}\phi_i B^i)^{-1}(1-\sum_{k=1}^{P}\Phi_k B^{ks})^{-1} 1-B)^{-d}(1-B^s)^{-D}$$

$$.(1-\sum_{j=1}^{q}\theta_j B^j)(1-\sum_{l=1}^{Q}\Theta_l B^{ls})\varepsilon_t+\sum_{i=1}^{n}(\omega_i X_{it})\Bigg). \qquad (10)$$

Therefore,

$$\begin{aligned}
\hat{L}(\upsilon_1) &= 1+\sum_{\eta=2}^{m} w_\eta \hat{L}(\upsilon_\eta)\, f\Bigg(\upsilon_\eta+K-\upsilon_1-(1-\sum_{i=1}^{p}\phi_i B^i)^{-1}(1-\sum_{k=1}^{P}\Phi_k B^{ks})^{-1} \\
&.(1-B)^{-d}(1-B^s)^{-D}(1-\sum_{j=1}^{q}\theta_j B^j)(1-\sum_{l=1}^{Q}\Theta_l B^{ls})\varepsilon_t+\sum_{i=1}^{n}(\omega_i X_{it})\Bigg) \\
&+\hat{L}(\upsilon_1)\Bigg[F\Bigg(K-\upsilon_1-(1-\sum_{i=1}^{p}\phi_i B^i)^{-1}(1-\sum_{k=1}^{P}\Phi_k B^{ks})^{-1} \\
&.(1-B)^{-d}(1-B^s)^{-D}(1-\sum_{j=1}^{q}\theta_j B^j)(1-\sum_{l=1}^{Q}\Theta_l B^{ls})\varepsilon_t+\sum_{i=1}^{n}(\omega_i X_{it})\Bigg) \\
&+w_1 f\Bigg(K-(1-\sum_{i=1}^{p}\phi_i B^i)^{-1}(1-\sum_{k=1}^{P}\Phi_k B^{ks})^{-1} \\
&.(1-B)^{-d}(1-B^s)^{-D}(1-\sum_{j=1}^{q}\theta_j B^j)(1-\sum_{l=1}^{Q}\Theta_l B^{ls})\varepsilon_t+\sum_{i=1}^{n}(\omega_i X_{it})\Bigg)\Bigg] \\
\hat{L}(\upsilon_2) &= 1+\sum_{\eta=2}^{m} w_\eta \hat{L}(\upsilon_\eta)\, f\Bigg(\upsilon_\eta+K-\upsilon_2-(1-\sum_{i=1}^{p}\phi_i B^i)^{-1}(1-\sum_{k=1}^{P}\Phi_k B^{ks})^{-1} \\
&.(1-B)^{-d}(1-B^s)^{-D}(1-\sum_{j=1}^{q}\theta_j B^j)(1-\sum_{l=1}^{Q}\Theta_l B^{ls})\varepsilon_t+\sum_{i=1}^{n}(\omega_i X_{it})\Bigg) \\
&+\hat{L}(\upsilon_1)\Bigg[F\Bigg(K-\upsilon_2-(1-\sum_{i=1}^{p}\phi_i B^i)^{-1}(1-\sum_{k=1}^{P}\Phi_k B^{ks})^{-1} \\
&.(1-B)^{-d}(1-B^s)^{-D}(1-\sum_{j=1}^{q}\theta_j B^j)(1-\sum_{l=1}^{Q}\Theta_l B^{ls})\varepsilon_t+\sum_{i=1}^{n}(\omega_i X_{it})\Bigg) \\
&+w_1 f\Bigg(\upsilon_1+K-\upsilon_2-(1-\sum_{i=1}^{p}\phi_i B^i)^{-1}(1-\sum_{k=1}^{P}\Phi_k B^{ks})^{-1} \\
&.(1-B)^{-d}(1-B^s)^{-D}(1-\sum_{j=1}^{q}\theta_j B^j)(1-\sum_{l=1}^{Q}\Theta_l B^{ls})\varepsilon_t+\sum_{i=1}^{n}(\omega_i X_{it})\Bigg)\Bigg] \\
&\vdots \qquad \vdots \qquad \vdots \\
\hat{L}(\upsilon_m) &= 1+\sum_{\eta=2}^{m} w_\eta \hat{L}(\upsilon_\eta)\, f\Bigg(\upsilon_\eta+K-\upsilon_m-(1-\sum_{i=1}^{p}\phi_i B^i)^{-1}(1-\sum_{k=1}^{P}\Phi_k B^{ks})^{-1} \\
&.(1-B)^{-d}(1-B^s)^{-D}(1-\sum_{j=1}^{q}\theta_j B^j)(1-\sum_{l=1}^{Q}\Theta_l B^{ls})\varepsilon_t+\sum_{i=1}^{n}(\omega_i X_{it})\Bigg) \\
&+\hat{L}(\upsilon_1)\Big[F\Big(K-\upsilon_m-(1-\sum_{i=1}^{p}\phi_i B^i)^{-1}(1-\sum_{k=1}^{P}\Phi_k B^{ks})^{-1} \\
&.(1-B)^{-d}(1-B^s)^{-D}(1-\sum_{j=1}^{q}\theta_j B^j)(1-\sum_{l=1}^{Q}\Theta_l B^{ls})\varepsilon_t+\sum_{i=1}^{n}(\omega_i X_{it})\Bigg) \\
&+w_1 f\Bigg(\upsilon_1+K-\upsilon_m-(1-\sum_{i=1}^{p}\phi_i B^i)^{-1}(1-\sum_{k=1}^{P}\Phi_k B^{ks})^{-1} \\
&.(1-B)^{-d}(1-B^s)^{-D}(1-\sum_{j=1}^{q}\theta_j B^j)(1-\sum_{l=1}^{Q}\Theta_l B^{ls})\varepsilon_t+\sum_{i=1}^{n}(\omega_i X_{it})\Bigg)\Bigg].
\end{aligned} \qquad (11)$$

The Equation (11) can be rewritten in matrix form as

$$\mathbf{L}_{m\times 1}=\mathbf{1}_{m\times 1}+\mathbf{R}_{m\times m}\mathbf{L}_{m\times 1}\Rightarrow \mathbf{L}_{m\times 1}=(\mathbf{I}_m-\mathbf{R}_{m\times m})^{-1}\mathbf{1}_{m\times 1} \qquad (12)$$

where $\mathbf{1}_{m\times 1}=[1,1,...,1]'$ is a vector of ones, $\mathbf{L}_{m\times 1}=\left[\hat{L}(\upsilon_1),\hat{L}(\upsilon_2),...,\hat{L}(\upsilon_m)\right]'\in \mathbb{R}^m$,

$$\mathbf{R}_{m\times m}=\begin{bmatrix} r_{11} & r_{12} & \cdots & r_{1m} \\ r_{21} & r_{22} & \cdots & r_{2m} \\ \vdots & \vdots & \ddots & \vdots \\ r_{m1} & r_{m2} & \cdots & r_{mm}\end{bmatrix},$$ where $r_{\eta\iota};\ \eta=1,2,....,m,$ and $\iota=1,2,....,m.$ A matrix $\mathbf{R}_{m\times m}$ with matrix entries given by

$$\begin{aligned}
r_{\eta\iota} &= w_\eta f\Bigg(\upsilon_\eta+K-\upsilon_\iota-(1-\sum_{i=1}^{p}\phi_i B^i)^{-1}(1-\sum_{k=1}^{P}\Phi_k B^{ks})^{-1} \\
&.(1-B)^{-d}(1-B^S)^{-D}(1-\sum_{j=1}^{q}\theta_j B^j)(1-\sum_{l=1}^{Q}\Theta_l B^{ls})\varepsilon_t+\sum_{i=1}^{n}(\omega_i X_{it})\Bigg) \\
&+F\Bigg(K-\upsilon_\eta-(1-\sum_{i=1}^{p}\phi_i B^i)^{-1}(1-\sum_{k=1}^{P}\Phi_k B^{ks})^{-1} \\
&.(1-B)^{-d}(1-B^s)^{-D}(1-\sum_{j=1}^{q}\theta_j B^j)(1-\sum_{l=1}^{Q}\Theta_l B^{ls})\varepsilon_t+\sum_{i=1}^{n}(\omega_i X_{it})\Bigg)
\end{aligned}$$

By substituting $\upsilon_\iota=\varphi$ into Equation (10), we obtain

$$\begin{aligned}
\hat{L}(\varphi) &= 1+\sum_{\eta=1}^{m} w_\eta \hat{L}(\upsilon_\eta)\, f\Bigg(\upsilon_\eta+K-\varphi-(1-\sum_{i=1}^{p}\phi_i B^i)^{-1}(1-\sum_{k=1}^{P}\Phi_k B^{ks})^{-1} \\
&.(1-B)^{-d}(1-B^s)^{-D}(1-\sum_{j=1}^{q}\theta_j B^j)(1-\sum_{l=1}^{Q}\Theta_l B^{ls})\varepsilon_t+\sum_{i=1}^{n}(\omega_i X_{it})\Bigg) \\
&+\hat{L}(\upsilon_1)F\Bigg(K-\varphi-(1-\sum_{i=1}^{p}\phi_i B^i)^{-1}(1-\sum_{k=1}^{P}\Phi_k B^{ks})^{-1}(1-B)^{-d}(1-B^s)^{-D} \\
&.(1-\sum_{j=1}^{q}\theta_j B^j)(1-\sum_{l=1}^{Q}\Theta_l B^{ls})\varepsilon_t+\sum_{i=1}^{n}(\omega_i X_{it})\Bigg).
\end{aligned} \qquad (13)$$

We can approximate the ARL by applying Equation (13) and substituting specific nodes and weights obtained through the NIE approach by utilizing the Gaussian quadrature, midpoint, trapezoidal, and Simpson's rules.

3.1 Gaussian (Gauss-Legendre) quadrature rule

Let $\hat{L}_G(\varphi)$ denote the ARL approximation obtained via the NIE approach using the Gauss-Legendre quadrature rule computed as follows:

$$\begin{aligned}
\hat{L}_G(\varphi) &= 1+\sum_{\eta=1}^{m} w_\eta \hat{L}(\upsilon_\eta)\, f\Bigg(\upsilon_\eta+K-\varphi-(1-\sum_{i=1}^{p}\phi_i B^i)^{-1}(1-\sum_{k=1}^{P}\Phi_k B^{ks})^{-1} \\
&.(1-B)^{-d}(1-B^s)^{-D}(1-\sum_{j=1}^{q}\theta_j B^j)(1-\sum_{l=1}^{Q}\Theta_l B^{ls})\varepsilon_t+\sum_{i=1}^{n}(\omega_i X_{it})\Bigg) \\
&+\hat{L}(\upsilon_1)F\Bigg(K-\varphi-(1-\sum_{i=1}^{p}\phi_i B^i)^{-1}(1-\sum_{k=1}^{P}\Phi_k B^{ks})^{-1}(1-B)^{-d}(1-B^s)^{-D} \\
&.(1-\sum_{j=1}^{q}\theta_j B^j)(1-\sum_{l=1}^{Q}\Theta_l B^{ls})\varepsilon_t+\sum_{i=1}^{n}(\omega_i X_{it})\Bigg).
\end{aligned} \qquad (14)$$

where $w_\eta = b/m$ and $\upsilon_\eta = b/m(\eta - 1/2)$; $\eta = 1,2,...,m.$

3.2 Midpoint Rule

Let $f(z)$ be a function defined on an interval $[0, b]$, which is divided into m, $\{[z_{\eta-1}, z_\eta], \eta = 1,2,...m\}$ subintervals of equal width $(U = b/m)$. The subintervals are spaced equally, $\{z_\eta = z_0 + \eta U,\ \eta = 0,1,2,...,m\}$, such that $z_0 = 0$ and $z_m = b$. The midpoint rule can be expressed in the following form:

$$M(f,U) = U\sum_{\iota=1}^{m} f\left(K + \left(\eta - \frac{1}{2}\right)U\right); \eta = 0,1,2,...,m \quad (15)$$

The integral of $f(z)$ from 0 to b can be approximated in the form of $\int_0^b f(z)dz \approx M(f,U)$. Therefore, the NIE approximation of the ARL via the midpoint rule can be written as

$$\begin{aligned}\hat{\mathrm{L}}_M(\varphi) &= 1 + \sum_{\eta=1}^{m} w_\eta \hat{\mathrm{L}}(\upsilon_\eta) f\Bigg(\upsilon_\eta + K - \varphi - (1-\sum_{i=1}^{p}\phi_i B^i)^{-1}(1-\sum_{k=1}^{P}\Phi_k B^{ks})^{-1} \\ &.(1-B)^{-d}(1-B^s)^{-D}(1-\sum_{j=1}^{q}\theta_j B^j)(1-\sum_{l=1}^{Q}\Theta_l B^{ls})\varepsilon_t + \sum_{i=1}^{n}(\omega_i X_{it})\Bigg) \\ &+\hat{\mathrm{L}}(\upsilon_1) F\Bigg(K - \varphi - (1-\sum_{i=1}^{p}\phi_i B^i)^{-1}(1-\sum_{k=1}^{P}\Phi_k B^{ks})^{-1}(1-B)^{-d}(1-B^s)^{-D} \\ &.(1-\sum_{j=1}^{q}\theta_j B^j)(1-\sum_{l=1}^{Q}\Theta_l B^{ls})\varepsilon_t + \sum_{i=1}^{n}(\omega_i X_{it})\Bigg). \end{aligned} \quad (16)$$

where $\upsilon_\eta = w_\eta(\eta - 1/2)$, and $w_\eta = b/m$; $\eta = 1,2,...,m.$

3.3 Trapezoidal Rule

The trapezoidal rule is defined as a function $f(z)$ on an interval $[0,b]$. It is divided into m subintervals, $\{[z_{\iota-1}, z_\eta], \eta = 1,2,...,m\}$, with a width $U = b/m$ and spaced equally, $\{z_\eta = z_0 + \eta U,\ \eta = 0,1,2,...,m\}$. Therefore, given that $z_0 = 0$ and $z_m = b$, the composite trapezoidal rule can be written as

$$T(f,U) = \frac{U}{2}\big(f(0) - f(b)\big) + U\sum_{\eta=1}^{m} f(z_\eta). \quad (17)$$

The integral of $f(z)$ from 0 to b can be approximately in the form of $\int_0^b f(z)dz \approx T(f,U)$. Therefore, the NIE approximation of the ARL via the trapezoidal rule $(\hat{\mathrm{L}}_T(\varphi))$ can be written in the form

$$\begin{aligned}\hat{\mathrm{L}}_T(\varphi) &= 1 + \sum_{\eta=1}^{m} w_\eta \hat{\mathrm{L}}(\upsilon_\eta) f\Bigg(\upsilon_\eta + K - \varphi - (1-\sum_{i=1}^{p}\phi_i B^i)^{-1}(1-\sum_{k=1}^{P}\Phi_k B^{ks})^{-1} \\ &.(1-B)^{-d}(1-B^s)^{-D}(1-\sum_{j=1}^{q}\theta_j B^j)(1-\sum_{l=1}^{Q}\Theta_l B^{ls})\varepsilon_t + \sum_{i=1}^{n}(\omega_i X_{it})\Bigg) \\ &+\hat{\mathrm{L}}(\upsilon_1) F\Bigg(K - \varphi - (1-\sum_{i=1}^{p}\phi_i B^i)^{-1}(1-\sum_{k=1}^{P}\Phi_k B^{ks})^{-1}(1-B)^{-d}(1-B^s)^{-D} \\ &.(1-\sum_{j=1}^{q}\theta_j B^j)(1-\sum_{l=1}^{Q}\Theta_l B^{ls})\varepsilon_t + \sum_{i=1}^{n}(\omega_i X_{it})\Bigg). \end{aligned} \quad (18)$$

where $\upsilon_\eta = \eta w_\eta$ and $w_\eta = b/m$; $\eta = 1,2,...,m-1,$
in other cases, $w_\eta = b/2m.$

3.4 Simpson's Rule

Let $[0,b]$ be partitioned into $2m$ equal subintervals $\{[z_{\eta-1}, z_\eta],\ \eta = 1,2,...,2m\}$ with width $U = b/2m$ and spaced equally $\{z_\eta = z_0 + \eta U, \quad \eta = 0,1,2,...,2m\}$. Therefore, given $z_0 = 0$ and $z_{2m} = b$, , the composite Simpson's functional can be written as

$$S(f,U) = \frac{U}{3}\big(f(0) - f(b)\big) + \frac{2U}{3}\sum_{\eta=1}^{m} f(z_{2\eta}) + \frac{4U}{3}\sum_{\eta=1}^{m} f(z_{2\eta-1}),$$
(19)

The integral of $f(z)$ from 0 to b is approximately in the form $\int_0^b f(z)dz \approx S(f,U)$. Therefore, the NIE approximation of the ARL via Simpson's rule $(\hat{\mathrm{L}}_s(\varphi))$ can be written in the form

$$\begin{aligned}\hat{\mathrm{L}}_s(\varphi) &= 1 + \sum_{\eta=1}^{m} w_\eta \hat{\mathrm{L}}(\upsilon_\eta) f\Bigg(\upsilon_\eta + K - \varphi - (1-\sum_{i=1}^{p}\phi_i B^i)^{-1}(1-\sum_{k=1}^{P}\Phi_k B^{ks})^{-1} \\ &.(1-B)^{-d}(1-B^s)^{-D}(1-\sum_{j=1}^{q}\theta_j B^j)(1-\sum_{l=1}^{Q}\Theta_l B^{ls})\varepsilon_t + \sum_{i=1}^{n}(\omega_i X_{it})\Bigg) \\ &+\hat{\mathrm{L}}(\upsilon_1) F\Bigg(K - \varphi - (1-\sum_{i=1}^{p}\phi_i B^i)^{-1}(1-\sum_{k=1}^{P}\Phi_k B^{ks})^{-1}(1-B)^{-d}(1-B^s)^{-D} \\ &.(1-\sum_{j=1}^{q}\theta_j B^j)(1-\sum_{l=1}^{Q}\Theta_l B^{ls})\varepsilon_t + \sum_{i=1}^{n}(\omega_i X_{it})\Bigg). \end{aligned} \quad (20)$$

where $\upsilon_\eta = \eta w_\eta$ and $w_\eta = \frac{4}{3}\left(\frac{b}{2m}\right)$; $\eta = 1,3,...,2m-1,$

$w_\eta = \frac{2}{3}\left(\frac{b}{2m}\right)$; $\eta = 2,4,...,2m-2,$

in other cases, $w_\eta = \frac{1}{3}\left(\frac{b}{2m}\right).$

4 Results and discussion

We proposed four NIE approaches for the structural design of the CUSUM control chart applied to the SAFIMAX(p, d, q, x)$\times$(P, D, Q)$_s$ model with exponential white noise. The optimal CUSUM control chart design parameters are (K, b), where K is 2.5, 2.75, or 3.00 and b is the decision interval (calculated using Equation (13) to yield ARL_0 values of 100, 370, and 500, respectively. Table 1 (Appendix) and Table 2 (Appendix) report the optimal calculated (K, b) configurations to achieve these target ARL_0 values. Since the ARL satisfies a Fredholm integral equation of the second kind, the numerical approximations produced by the NIE methods converge to the true ARL solution as the number of discretization nodes increases, with convergence rates governed by the underlying quadrature schemes. In the implementation, all four NIE approaches were evaluated using $m = 500$ nodes on the interval [0, b], which was found to be sufficient for accurately approximating the target ARL_0 values.

To complement the theoretical convergence properties, an empirical convergence study was also conducted by computing ARL values for increasing numbers of nodes m. The results, reported in Table 1 (Appendix) and Table 2 (Appendix), exhibit monotone stabilization of the ARL approximations as m increases, indicating numerical convergence and supporting the theoretical accuracy of the proposed NIE methods.

In addition, the in-control process using the exponent parameter $(\alpha = \alpha_0)$ was set to 1, with $\varepsilon_t \sim Exp(\alpha_0 = 1)$. the out-of-control parameter $(\alpha = \alpha_1)$ was set to $\alpha_1 = \alpha_0(1+\delta)$, with $\alpha_1 > \alpha_0$. The shift sizes (δ) were in the set $\delta = \{0.75, 1.50, 2.25, 3.00, 3.75, 4.50\}$.

Percentage relative deviation (%Dev) can be used to evaluate detection sensitivity for mean shifts of varying magnitudes, using the following formula:

$$\%Dev = \left| \frac{\hat{L}_1(\varphi) - \hat{L}_0(\varphi)}{\hat{L}_0(\varphi)} \right| \times 100\%, \qquad (21)$$

where $\hat{L}_1(\varphi)$ and $\hat{L}_0(\varphi)$ are NIE-based ARL approximations forARL_1 and ARL_0, respectively.

Interpretation: The lowest $\%Dev$ value signifies the shift size that can be detected with the highest sensitivity.

Across all process mean change levels, the ARL_1 results for the four NIE-based approaches reveal that Simpson's rule yielded the lowest values, followed by the midpoint, trapezoidal, and Gaussian quadrature rules, respectively, in all of the scenarios studied (Table 1 (Appendix) and Table 2 (Appendix)).

However, the midpoint rule had the shortest computation processing time (450–560 s), followed closely by the Gaussian quadrature and trapezoid rules. In contrast, Simpson's Rule required a much longer computation time (3,990–4,240 s). With acceptable ARL results and a fast computation time, the midpoint rule-based NIE method is ideal for applications that require a quick response, followed by the trapezoidal and Gauss-Legendre quadrature rule-based NIE methods. Furthermore, the midpoint rule also showed the lowest percentage deviation (%Dev) at a change of magnitude of 0.75. This indicates that the process mean shift size could be detected with the highest sensitivity and is appropriate for setting control limits.

Overall, these methods vary in terms of accuracy and computational efficiency, and the choice of an appropriate method depends on the specific requirements of the analysis. In conclusion, the midpoint rule is the most appropriate choice for approximating the ARL of a SARFIMAX process on a CUSUM control chart in this simulation context.

5 Real-Data application

We used 65 monthly observations of Gold Fabricated Futures – 1 (XAU-F-TH), [31], with the XAU/THB exchange rate, [32], as an exogenous variable over the monthly period from May 2019 to September 2024. SARFIMAX model fitting was performed using the statistical software package Eviews. The estimated parameters, along with their standard errors and corresponding p-values for the best-fitted SAFIMAX(p, d, q)$\times$(P, D, Q)$_s$
model, are provided in Table 1.

The SAFIMAX $(p, d, q)\times(P, D, Q)_s$ model was a good fit for the data, as evidenced by the estimated parameters having *p*-values less than 0.05. The process being long memory was confirmed by the fact that the conditions $0<(d+D)<0.5$ and $0<D<0.5$ were satisfied. To assess the accuracy of the model, the fitted values were plotted together with the actual data (Figure 1). Thereby, the process monitored by the CUSUM control chart fitted a SAFIMAX(1, 0.0389, 1) $\times$(1, 0.4612, 1)$_{12}$ model, with coefficient parameters $\phi_1=0.9999$, $\Phi_1=0.4111$, $\theta_1=-0.0284$, $\Theta_1=0.9999$, $\omega_1=1.8552$.

Table 1 Parameter estimates for the long-memory SARFIMAX model.

Parameters	Estimate	Std.Error	t-Statistic	p-Value
D	0.4612	0.0341	13.5088	0.0000
X_{it}	1.8552	0.8267	2.2441	0.0287
d	0.0389	0.0006	70.4258	0.0000
AR(1)	0.9999	0.4221	2.3694	0.0212
SAR(12)	0.4111	0.0045	90.8779	0.0000
MA(1)	-0.0284	0.0004	-78.2626	0.0000
SMA(12)	0.9999	0.0253	39.4932	0.0000
Log likelihood			-514.392	
AIC			16.0428	

Source: Calculations conducted by the authors using Wolfram Mathematica 8.

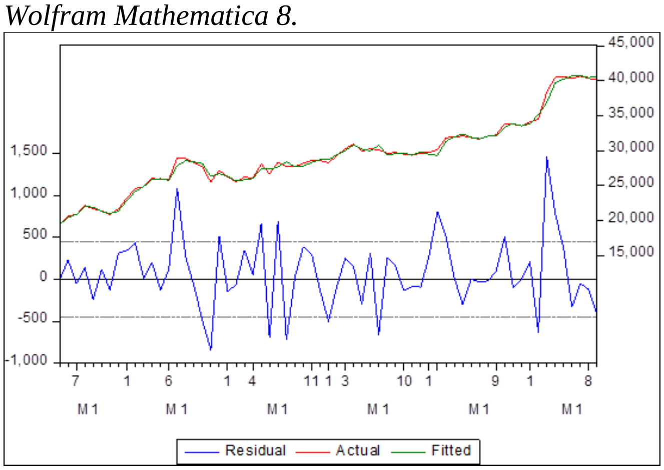

Fig. 1: Graphical representation of real and fitted data, along with a plot of the residuals for the real data.
Source: Calculations conducted by the authors using Wolfram Mathematica 8.

Table 2. One-sample Kolmogorov-Smirnov testing of the assumption that the white noise follows an exponential distribution.

Statistic	Value
Observations	65[c]
Exponential Parameter (Mean)[a,b]	337.8129
Kolmogorov-Smirnov	0.5876
Asymp. Sig. (2-tailed)	0.8802

a. Test Distribution is Exponential.
b. Calculated from data.
c. There are 28 observations outside the specified distribution range. These values are skipped.
Source: Authors' calculations using IBM SPSS Statistics.

Table 2 reports the Kolmogorov-Smirnov testing results (observations = 65) to assess whether the residuals (white noise) follow an exponential distribution (α_0 = 337.8129). The Kolmogorov-Smirnov statistic value was 0.5876, with an asymptotic two-tailed significance of 0.8802. Since the p-value exceeds 0.05, the null hypothesis is not rejected. Therefore, the white noise can be assumed to follow an exponential distribution.

Thus, the fitted model can be expressed as

$$(1-0.9999B)(1-0.4111B^{12})(1-B)^{0.0389}(1-B^{12})^{0.4612}Y_t = (1+0.0284B)(1-0.9999B^{12})\varepsilon_t+1.8552X_{1t}, \tag{22}$$

where $\varepsilon_t \sim Exp(337.8129)$.

The results for the simulation study indicate that the CUSUM control chart with $K = 2.5$ and decision interval values b = 396.544, 498.917 (calculated using Equation (13)) provides the optimal configuration, corresponding to ARL_0 values of 370 and 500, respectively (Table 3 (Appendix)). These findings are consistent with the numerical results in Table 1 (Appendix) and Table 2 (Appendix).

The ARL_1 results obtained from the four NIE-based methods evaluated at various levels of process mean shifts were similar and consistent with the simulation study results. Regarding computational efficiency, the midpoint rule required the least amount of processing time, followed by the Gaussian quadrature, trapezoidal, and Simpson's rules, in that order. Furthermore, the midpoint rule exhibited the smallest percentage deviation (%Dev) at a change magnitude of 0.75. As previously noted, the midpoint rule demonstrates excellent performance in detecting shifts in real-data applications and is suitable for establishing control limits.

The CUSUM control limits were calibrated to achieve in-control ARL values of 370 (UCL = 396.544, CL = 337.8129, LCL = 0) and 500 (UCL = 498.917, CL = 337.8129, LCL = 0). As illustrated in Figure 1 (Appendix), the first out-of-control signal occurred at observation 7 when ARL_0 = 370 and at observation 11 when ARL_0 = 500. This highlights the substantial impact of setting ARL_0 on the CUSUM control chart sensitivity, underscoring the importance of selecting appropriate parameter values to optimize detection performance.

6 Conclusions

We proposed performance evaluation measures for the CUSUM control chart designed to detect small-to-moderate upward shifts in the mean of a SARFIMAX time series. To this end, we employed the NIE approach based on the Gauss-Legendre quadrature, trapezoidal, Simpson's, or midpoint rule. The performance of methods for a SARFIMAX process on a CUSUM control chart was assessed via the ARL, percentage relative deviation (%Dev), and computational efficiency. The ARL_1 results obtained from the four proposed NIE-based methods demonstrated their comparable effectiveness in detecting changes across a wide range of processes. However, in terms of computational efficiency, the midpoint rule yielded the best overall performance while the Simpson's rule method exhibited the worst. Furthermore, the %Dev obtained using the midpoint rule demonstrated high sensitivity in detecting small-to-moderate upward shifts in the SARFIMAX process mean, with setting $K = 2.5$ for the control chart being the most efficient across all ARL_0 values.

The focus of this study was solely on the upper-side CUSUM control chart for a SAFIMAX$(p, d, q)\times(P, D, Q)_s$ time series. However, the midpoint rule can be applied to other time series and memory-type control charts (e.g., EWMA). In addition, we exclusively concentrated on detecting upward shifts in the process mean. However, investigating shifts in the process mean on a two-sided CUSUM or mixed EWMA-CUSUM control chart for some applications warrants further study.

In conclusion, we recommend using the proposed midpoint rule to assess the CUSUM control chart performance in terms of the ARL of a SARFIMAX process with exponential white noise.

Acknowledgement:
This research budget was allocated by Nation Science, Research, and Innovation Fund (NSRF), and King Mongkut's University of Technology North Bangkok under contract no. KMUTNB-FF-68-B-45.

Declaration of Generative AI and AI-assisted technologies in the writing process

During the preparation of this work, the author used QuillBot in order to study the source and importance of research. After using this tool/service, the author reviewed and edited the content as needed and took full responsibility for the content of the publication.

References:

[1] Montgomery, D. C., *Introduction to Statistical Quality Control*, Chichester: Wiley, New York, 5th edition, 2005. https://books.google.gr/books?hl=el&lr=&id=oh7zDwAAQBAJ&oi=fnd&pg=PA2&ots=DsDwg5G68z&sig=EdrYBuwv26SktNK-JsW1Zf4ljso&redir_esc=y#v=onepage&q&f=false [Access Date: 01/01/2026]

[2] Page, E. S. , Continuous inspection schemes, *Biometrika*, Vol. 41, No.1-2, 1954, pp. 100-115. DOI: https://doi.org/10.2307/2333009

[3] Roberts, S. W. , Control Chart Test Based on Geometric Moving Averages, *Technometrics*, Vol 1, 2000, pp. 97-101. DOI: https://doi.org/10.1080/00401706.2000.10485986

[4] Sasikumar, R. and Devi, S.B., Cumulative sum charts and its healthcare applications: A systematic review, *Sri Lankan Journal of Applied Statistics*, Vol. 15, No. 1, 2014, pp. 47–56. DOI: http://dx.doi.org/10.4038/sljastats.v15i1.6793

[5] Yule, G.U., Why do we sometimes get nonsense-correlations between time-series?, Journal of the Royal Statistical Society, Vol. 89, 1926, pp. 1–63. DOI: https://doi.org/10.2307/2341482

[6] Slutsky, E., The summation of random causes as the source of cyclic processes, Econometrica, Vol. 5, 1937, pp. 105–146. DOI: https://doi.org/10.2307/1907241

[7] Box, G. E. P. and Jenkins, G. M., *Time series analysis: forecasting and control Holden Day*, San Francisco, CA, 1976.

https://books.google.gr/books?hl=en&lr=&id=dFKUIS_puRcC&oi=fnd&pg=PA161&ots=4v3Yizw4g8&sig=me7XQJxDhBcZnQFMvXYEErgUME&redir_esc=y#v=onepage&q&f=false [Access Date: 01/01/2026]

[8] Granger C. W. J. and Joyeux, R., An Introduction to Long Memory Time Series Models and Fractional Differencing, *Journal of Time Series Analysis*, Vol.1, No.1, 1980, pp. 15-29. DOI: https://doi.org/10.1111/j.1467-9892.1980.tb00297.x

[9] Hosking J. R. M., Fractional differencing, *Biometrika*, Vol.68, No.1, 1981, pp. 165-176. DOI: https://doi.org/10.2307/2335817

[10] Beran, J., *Statistics for long-memory processes*, Chapman and Hall, New York, 1st edition, 1994. DOI: https://doi.org/10.1201/9780203738481

[11] Chan, N.H. and Palma, W., Estimation of long-memory time series models: A survey of different likelihood-based methods, *Advances in Econometrics*, Vol. 20, 2006, pp. 89–121. DOI: https://doi.org/10.1016/S0731-9053(05)20023-3

[12] Beran, J., Feng, Y., Ghosh, S. and Kulik, R., *Long-memory processes—probabilistic properties and statistical methods*, Springer, New York, 2013. https://doi.org/10.1007/978-3-642-35512-7

[13] Yashchin, E. Performance of CUSUM control schemes for Serially correlate observations, *Technometrics*, Vol. 35, No.1, 1993, pp. 37-52. DOI: https://doi.org/10.2307/1269288

[14] Zhang, L. and Busababodhin, P., The ARIMA(p,d,q) on upper sided of CUSUM procedure, *Lobachevskii Journal of Mathematics*, Vol. 39, 2018, pp. 424–432. DOI: https://doi.org/10.1134/S1995080218030216

[15] Areepong, Y. and Peerajit, W., Integral equation solutions for the average run length for monitoring shifts in the mean of a generalized seasonal ARFIMAX(P, D, Q, r)$_s$ process running on a CUSUM control chart, *PLoS ONE*, Vol. 17, No. 2, 2022, pp. e0264283. DOI: https://doi.org/10.1371/journal.pone.0264283

[16] Montanari, A., Rosso, R. and Taqqu, M.S., A seasonal fractional ARIMA model applied to Nile river monthly flows at Aswan, *Water Resources Research*, Vol. 36, No. 5, 2000, pp. 1249–1259. DOI: https://doi.org/10.1029/2000WR900012

[17] Porter-Hudak, S., An application of the seasonal fractionally differenced model to the monetary aggregates, *Journal of the American Statistical Association*, Vol. 85, 1990, pp. 338–344. DOI: https://doi.org/10.2307/2289769

[18] Ray, B.K., Modeling long-memory processes for optimal long-range prediction, *Journal of Time Series Analysis*, Vol. 14, No. 5, 1993, pp. 511–525. DOI: https://doi.org/10.1111/j.1467-9892.1993.tb00161.x

[19] Hassler, U. and Wolters, J., Long memory in inflation rates: International evidence, *Journal of Business and Economic Statistics*, Vol. 13, pp. 37–45, 1995. DOI: https://doi.org/10.2307/1392519

[20] Ooms, M., *Flexible Seasonal Long Memory and Economic Time Series* (Technical Report EI-9515/A). Rotterdam, The Netherlands: Erasmus University Rotterdam, Econometric Institute, 1995. https://econpapers.repec.org/paper/emseureir/1351.htm [Access Date: 01/01/2026]

[21] Ebens H., *Realized stock index volatility*, Department of Economics, Johns Hopkins University. 1999. https://ideas.repec.org/p/jhu/papers/420.html [Access Date: 01/01/2026]

[22] Degiannakis, S., ARFIMAX and ARFIMAX-TARCH realized volatility modeling, Journal of Applied Statistics, Vol. 35, No. 10, 2008, pp. 1169–1180. DOI: https://doi.org/10.1080/02664760802271017

[23] Ibazizen, M. and Fellag, H., Bayesian estimation of an AR(1) process with exponential white noise, *Statistics*, Vol.37, No.5, pp. 365-372, 2003. https://doi.org/10.1080/0233188031000078042

[24] Suparman, S. , A new estimation procedure using a reversible jump MCMC algorithm for AR models of exponential white noise, *International Journal of GEOMATE*, Vol.15, No.49, pp. 85-91, 2018. DOI: https://doi.org/10.21660/2018.49.3622

[25] Peerajit, W. Gauss–Legendre Numerical Integrations for Average Run Length Running on EWMA Control Chart with Fractionally Integrated MAX Process, *WSEAS Transactions on Mathematics*, Vol. 23, pp. 579–590, 2024. https://doi.org/10.37394/23206.2024.23.61

[26] Farah, G.N. and Lindner, B., Exponentially distributed noise—its correlation function and its effect on nonlinear dynamic, *Journal of Physics A: Mathematical and Theoretical*, Vol.

54, No. 3, pp. 035003, 2020. DOI: https://doi.org/10.1088/1751-8121/abd2fd

[27] Somran, S., Areepong, Y. and Sukparungsee, S., Analytic and numerical solutions of ARL of CUSUM procedure for exponentially distributed observations, *Thailand Statistician*, Vol. 14, No. 1, pp. 83–91, 2016. https://ph02.tci-thaijo.org/index.php/thaistat/article/view/47321 [Access Date: 01/01/2026]

[28] Buranapol, P., Phanyaem, S., Phanyaem, S. and Areepong, Y., Average run length of CUSUM control chart for SARX(P, 1)$_L$ model using numerical integral equation method, *The Journal of Applied Science*, Vol. 21, No. 1, 2022, pp. 1–17. https://ph01.tci-thaijo.org/index.php/JASCI/article/view/246470 [Access Date: 01/01/2026]

[29] Bualuang, Y. and Peerajit, W., Performance of the CUSUM control chart using approximation to ARL for long-memory fractionally integrated autoregressive process with exogenous variable, *Applied Science and Engineering Progress*, Vol. 16, No. 2, pp. 5917, 2023. DOI: www.doi.org/10.14416/j.asep.2022.05.003

[30] Wieringa, J.E., *Statistical Process Control for Serially Correlated Data* (Doctoral thesis). University of Groningen, The Netherlands, 1999. ISBN: 90-72591-63-1 https://research.rug.nl/en/publications/statistical-process-control-for-serially-correlated-data/ [Access Date: 01/01/2026]

[31] *(text in Thai)* Gold fabricated Futures - 1 (XAU-F-TH). (2019) [Online]. Available: https://th.investingcom/commodities [Access Date: 01/01/2026]

[32] *(text in Thai)* USD to THB exchange rate. (2019). [Online]. Available: https://th.investing.com/currencies [Access Date: 01/01/2026]

Contribution of Individual Authors to the Creation of a Scientific Article (Ghostwriting Policy)

- Conceptualization: Wilasinee Peerajit.
- Data curation: Wilasinee Peerajit.
- Formal analysis: Wilasinee Peerajit.
- Funding acquisition: Wilasinee Peerajit.
- Investigation: Wilasinee Peerajit.
- Methodology: Wilasinee Peerajit.
- Software: Wilasinee Peerajit.
- Validation: Wilasinee Peerajit.
- Writing – original draft: Wilasinee Peerajit.
- Writing – review and editing: Wilasinee Peerajit

The authors contributed in the present research, at all stages from the formulation of the problem to the final findings and solution.

Sources of Funding for Research Presented in a Scientific Article or Scientific Article Itself

The author gratefully acknowledges the editor and referees for their valuable comments and suggestions which greatly improve this paper. This research budget was allocated by Nation Science, Research and Innovation Fund (NSRF), and King Mongkut's University of Technology North Bangkok under contract no. KMUTNB-FF-68-B-45.

Conflict of Interest

The authors declare no conflict of interest.

APPENDIX

Table 1. The ARL_1 results for the four NIE-based approaches for the long-memory $\mathrm{SARFIMAX}(1,0.1,1)\times(1,0.2,1)_{12}$ model on a CUSUM control chart.

δ	ARL$_0$ = 100														
	(K = 2.5, b = 2.9185125)				%Dev	(K = 2.75, b = 2.547573)				%Dev	(K = 3.0, b = 2.22648)				%Dev
	$\hat{L}_G(\varphi)$	$\hat{L}_M(\varphi)$	$\hat{L}_T(\varphi)$	$\hat{L}_S(\varphi)$		$\hat{L}_G(\varphi)$	$\hat{L}_M(\varphi)$	$\hat{L}_T(\varphi)$	$\hat{L}_S(\varphi)$		$\hat{L}_G(\varphi)$	$\hat{L}_M(\varphi)$	$\hat{L}_T(\varphi)$	$\hat{L}_S(\varphi)$	
0.75	11.550	11.399	11.467	11.349	88.60%	11.956	11.867	11.909	11.826	88.13%	12.283	12.228	12.257	12.196	87.77%
	(499)	(453)	(536)	(4,114)		(505)	(460)	(538)	(4,109)		(495)	(458)	(540)	(4,016)	
1.50	5.179	5.150	5.163	5.141	94.85%	5.315	5.296	5.305	5.289	94.70%	5.436	5.423	5.430	5.418	94.58%
	(511)	(455)	(535)	(4,240)		(505)	(459)	(542)	(4,174)		(493)	(460)	(537)	(3,993)	
2.25	3.457	3.446	3.451	3.443	96.55%	3.510	3.502	3.506	3.500	96.50%	3.564	3.559	3.561	3.557	96.44%
	(505)	(455)	(535)	(4,111)		(494)	(463)	(536)	(4205)		(494)	(459)	(536)	(4,004)	
3.00	2.711	2.705	2.708	2.704	97.30%	2.732	2.729	2.731	2.727	97.27%	2.760	2.757	2.759	2.756	97.24%
	(495)	(455)	(536)	(4128)		(492)	(463)	(536)	(4,139)		(495)	(459)	(539)	(3,996)	
3.75	2.304	2.301	2.302	2.300	97.70%	2.312	2.310	2.311	2.309	97.69%	2.327	2.325	2.326	2.325	97.68%
	(499)	(452)	(536)	(4,142)		(499)	(462)	(537)	(4,145)		(507)	(459)	(537)	(3,988)	
4.50	2.051	2.049	2.049	2.048	97.95%	2.052	2.050	2.051	2.050	97.95%	2.060	2.059	2.059	2.058	97.94%
	(493)	(500)	(536)	(4,201)		(495)	(459)	(534)	(4,280)		(496)	(459)	(534)	(3,986)	
δ	ARL$_0$ = 370														
	(K = 2.5, b = 4.5574738)				%Dev	(K = 2.75, b = 4.042056)				%Dev	(K = 3.0, b = 3.65309)				%Dev
0.75	20.721	19.176	19.788	18.946	94.82%	22.531	21.662	22.025	21.430	94.15%	23.816	23.280	23.515	23.069	93.71%
	(494)	(496)	(538)	(4,143)		(495)	(461)	(551)	(4,324)		(496)	(461)	(536)	(3,982)	
1.50	7.427	7.246	7.320	7.219	98.04%	7.953	7.838	7.887	7.811	97.88%	8.361	8.282	8.318	8.258	97.76%
	(494)	(457)	(535)	(4,113)		(494)	(458)	(536)	(4,205)		(498)	(458)	(537)	(3,986)	
2.25	4.602	4.549	4.571	4.540	98.77%	4.782	4.746	4.762	4.738	98.72%	4.944	4.918	4.930	4.911	98.67%
	(495)	(456)	(540)	(4,138)		(493)	(459)	(535)	(4,149)		(506)	(460)	(536)	(3,987)	
3.00	3.468	3.446	3.455	3.441	99.07%	3.536	3.520	3.527	3.516	99.05%	3.611	3.600	3.605	3.597	99.03%
	(494)	(455)	(537)	(4,130)		(493)	(460)	(533)	(4,126)		(495)	(458)	(539)	(4,167)	
3.75	2.869	2.857	2.862	2.854	99.23%	2.892	2.883	2.887	2.881	99.22%	2.930	2.924	2.927	2.922	99.21%
	(494)	(456)	(536)	(4,126)		(494)	(459)	(537)	(4,151)		(497)	(457)	(536)	(4,662)	
4.50	2.501	2.494	2.497	2.492	99.33%	2.504	2.498	2.501	2.497	99.32%	2.524	2.519	2.521	2.518	99.32%
	(492)	(452)	(537)	(4,121)		(493)	(461)	(546)	(4,143)		(496)	(459)	(537)	(3,979)	
δ	ARL$_0$ = 500														
	(K = 2.5, b = 4.9674795)				%Dev	(K = 2.75, b = 4.397021)				%Dev	(K = 3.0, b = 3.987543)				%Dev
0.75	23.294	20.710	21.700	20.415	95.86%	25.858	24.431	25.013	24.108	95.11%	27.567	26.690	27.065	26.383	94.66%
	(494)	(455)	(535)	(4,144)		(504)	(459)	(538)	(4,161)		(496)	(458)	(536)	(3,971)	
1.50	7.874	7.609	7.715	7.576	98.48%	8.604	8.437	8.507	8.404	98.31%	9.137	9.022	9.073	8.990	98.20%
	(502)	(456)	(540)	(4,170)		(496)	(458)	(535)	(4,183)		(495)	(459)	(538)	(3,958)	
2.25	4.837	4.762	4.792	4.752	99.05%	5.077	5.029	5.049	5.019	98.99%	5.283	5.248	5.264	5.239	98.95%
	(496)	(451)	(537)	(4,112)		(492)	(461)	(534)	(4,136)		(492)	(460)	(536)	(4,001)	
3.00	3.633	3.601	3.614	3.596	99.28%	3.721	3.700	3.709	3.695	99.26%	3.815	3.799	3.806	3.795	99.24%
	(495)	(456)	(539)	(4,127)		(495)	(459)	(536)	(4,104)		(496)	(460)	(539)	(3,958)	
3.75	2.997	2.980	2.987	2.977	99.40%	3.026	3.014	3.019	3.012	99.40%	3.073	3.064	3.068	3.062	99.39%
	(494)	(455)	(536)	(4,130)		(496)	(459)	(537)	(3,985)		(493)	(459)	(535)	(3,955)	
4.50	2.605	2.596	2.600	2.594	99.48%	2.608	2.601	2.604	2.600	99.48%	2.632	2.627	2.629	2.626	99.47%
	(496)	(454)	(537)	(4,105)		(495)	(460)	(536)	(4,221)		(496)	(459)	(541)	(3,955)	

Note that: The computational times in parentheses are in seconds.
Source: created by the authors.

Table 2. The ARL_1 results for the four NIE-based approaches for the long-memory $\mathrm{SARFIMAX}(1,0.1,1)\times(1,0.2,2)_{12}$ model on a CUSUM control chart.

δ	(K = 2.5, b = 2.6448797)				%Dev	(K = 2.75, b = 2.3130120)				%Dev	(K = 3.0, b = 2.012720)				%Dev
	ARL_0 = 100														
	$\hat{L}_G(\varphi)$	$\hat{L}_M(\varphi)$	$\hat{L}_T(\varphi)$	$\hat{L}_S(\varphi)$		$\hat{L}_G(\varphi)$	$\hat{L}_M(\varphi)$	$\hat{L}_T(\varphi)$	$\hat{L}_S(\varphi)$		$\hat{L}_G(\varphi)$	$\hat{L}_M(\varphi)$	$\hat{L}_T(\varphi)$	$\hat{L}_S(\varphi)$	
0.75	11.851	11.748	11.797	11.705	88.25%	12.198	12.136	12.168	12.101	87.86%	12.479	12.440	12.462	12.414	87.56%
	(520)	(487)	(552)	(4119)		(512)	(478)	(548)	(3998)		(536)	(479)	(544)	(4056)	
1.50	5.278	5.257	5.267	5.249	94.74%	5.404	5.389	5.397	5.383	94.61%	5.513	5.503	5.509	5.499	94.50%
	(510)	(499)	(555)	(4015)		(515)	(471)	(551)	(3998)		(533)	(486)	(549)	(3985)	
2.25	3.494	3.486	3.490	3.484	96.51%	3.549	3.543	3.546	3.541	96.46%	3.601	3.597	3.599	3.595	96.40%
	(540)	(500)	(554)	(4002)		(513)	(467)	(554)	(4004)		(536)	(475)	(550)	(3992)	
3.00	2.725	2.721	2.723	2.720	97.28%	2.752	2.749	2.751	2.748	97.25%	2.780	2.778	2.779	2.777	97.22%
	(523)	(511)	(558)	(4050)		(515)	(472)	(577)	(4026)		(533)	(470)	(546)	(3989)	
3.75	2.309	2.306	2.308	2.306	97.69%	2.322	2.321	2.321	2.320	97.68%	2.339	2.337	2.338	2.337	97.66%
	(523)	(495)	(553)	(4011)		(512)	(468)	(556)	(4019)		(530)	(469)	(548)	(4062)	
4.50	2.051	2.049	2.050	2.048	97.95%	2.057	2.056	2.057	2.056	97.94%	2.067	2.066	2.067	2.066	97.93%
	(531)	(501)	(553)	(4023)		(515)	(471)	(549)	(4021)		(532)	(470)	(552)	(4083)	
δ	**ARL_0 = 370**														
	(K = 2.5, b = 4.1679079)				%Dev	(K = 2.75, b = 3.754802)				%Dev	(K = 3.0, b = 3.408819)				%Dev
0.75	22.099	21.090	21.506	20.857	94.30%	23.489	22.879	23.143	22.661	93.82%	24.568	24.179	24.357	23.988	93.47%
	(526)	(478)	(551)	(4020)		(513)	(470)	(575)	(4018)		(534)	(474)	(547)	(4050)	
1.50	7.821	7.692	7.747	7.666	97.92%	8.255	8.168	8.206	8.143	97.79%	8.612	8.550	8.579	8.528	97.69%
	(519)	(482)	(555)	(4002)		(514)	(480)	(577)	(4008)		(540)	(473)	(546)	(4047)	
2.25	4.733	4.694	4.711	4.686	98.73%	4.900	4.872	4.885	4.865	98.68%	5.050	5.030	5.040	5.023	98.64%
	(516)	(474)	(561)	(4066)		(496)	(470)	(590)	(4003)		(561)	(487)	(557)	(4043)	
3.00	3.515	3.498	3.505	3.494	99.05%	3.590	3.578	3.583	3.574	99.03%	3.665	3.656	3.660	3.653	99.01%
	(513)	(481)	(556)	(4165)		(489)	(470)	(583)	(3993)		(555)	(482)	(550)	(4035)	
3.75	2.883	2.874	2.878	2.871	99.22%	2.919	2.912	2.915	2.910	99.21%	2.960	2.955	2.958	2.953	99.20%
	(518)	(513)	(555)	(4069)		(487)	(470)	(572)	(3994)		(536)	(470)	(546)	(4037)	
4.50	2.500	2.494	2.497	2.493	99.33%	2.517	2.513	2.515	2.512	99.32%	2.541	2.538	2.540	2.537	99.31%
	(516)	(534)	(552)	(4044)		(485)	(477)	(576)	(4032)		(546)	(474)	(548)	(4033)	
δ	**ARL_0 = 500**														
	(K = 2.5, b = 4.5323420)				%Dev	(K = 2.75, b = 4.093624)				%Dev	(K = 3.0, b = 3.734823)				%Dev
0.75	25.269	23.611	24.278	23.289	95.28%	27.136	26.136	26.558	25.823	94.77%	28.554	27.918	28.199	27.633	94.42%
	(520)	(478)	(557)	(4027)		(489)	(467)	(576)	(4051)		(536)	(471)	(545)	(4019)	
1.50	8.428	8.241	8.319	8.208	98.35%	9.000	8.873	8.928	8.840	98.23%	9.458	9.368	9.409	9.338	98.13%
	(515)	(482)	(551)	(4075)		(517)	(469)	(575)	(4027)		(506)	(473)	(558)	(4027)	
2.25	5.014	4.960	4.983	4.950	99.01%	5.228	5.190	5.207	5.180	98.96%	5.416	5.388	5.401	5.379	98.92%
	(516)	(483)	(552)	(4019)		(507)	(469)	(580)	(4028)		(516)	(477)	(551)	(4038)	
3.00	3.695	3.671	3.681	3.667	99.27%	3.789	3.772	3.779	3.767	99.25%	3.881	3.868	3.874	3.864	99.23%
	(514)	(478)	(560)	(3991)		(508)	(472)	(568)	(4029)		(511)	(477)	(556)	(4028)	
3.75	3.014	3.002	3.007	2.999	99.40%	3.059	3.050	3.054	3.047	99.39%	3.109	3.102	3.105	3.100	99.38%
	(514)	(478)	(551)	(4024)		(504)	(467)	(571)	(4060)		(507)	(470)	(548)	(4051)	
4.50	2.604	2.597	2.600	2.595	99.48%	2.625	2.619	2.622	2.618	99.48%	2.654	2.649	2.651	2.648	99.47%
	(515)	(480)	(552)	(4002)		(508)	(469)	(576)	(4028)		(507)	(473)	(545)	(4030)	

Note that: The computational times in parentheses are in seconds.
Source: created by the authors.

Table 3 The ARL results for the four NIE approaches on one-sided CUSUM with real data fitted to a SARFIMAX model.

δ	$ARL_0 = 370$					$ARL_0 = 500$				
	(K = 2.5, b = 396.544)				(%Dev)	(K = 2.5, b = 498.917)				(%Dev)
	$\hat{L}_G(\varphi)$	$\hat{L}_M(\varphi)$	$\hat{L}_T(\varphi)$	$\hat{L}_S(\varphi)$		$\hat{L}_G(\varphi)$	$\hat{L}_M(\varphi)$	$\hat{L}_T(\varphi)$	$\hat{L}_S(\varphi)$	
0.75	29.063	**29.041**	29.060	29.023	92%	34.349	**34.313**	34.343	34.276	93%
	(477)	**(442)**	(517)	(4,029)		(481)	**(442)**	(524)	(3,963)	
1.50	10.515	**10.509**	10.514	10.507	97%	11.781	**11.773**	11.780	11.767	98%
	(480)	**(443)**	(515)	(4,018)		(476)	**(445)**	(564)	(3,957)	
2.25	6.093	**6.091**	6.093	6.090	98%	6.640	**6.637**	6.640	6.635	99%
	(479)	**(444)**	(516)	(4,051)		(482)	**(442)**	(515)	(3,974)	
3.00	4.338	**4.336**	4.337	4.336	99%	4.648	**4.647**	4.648	4.646	99%
	(477)	**(441)**	(514)	(3,998)		(486)	**(448)**	(524)	(3,970)	
3.75	3.439	**3.439**	3.439	3.438	99%	3.645	**3.644**	3.645	3.643	99%
	(477)	**(446)**	(521)	(4,030)		(480)	**(443)**	(517)	(3,969)	
4.50	2.906	**2.906**	2.906	2.905	99%	3.055	**3.055**	3.055	3.054	99%
	(479)	**(442)**	(515)	(4,028)		(479)	**(443)**	(523)	(4,068)	

Note that: The computational times in parentheses are in seconds.
Source: created by the authors.

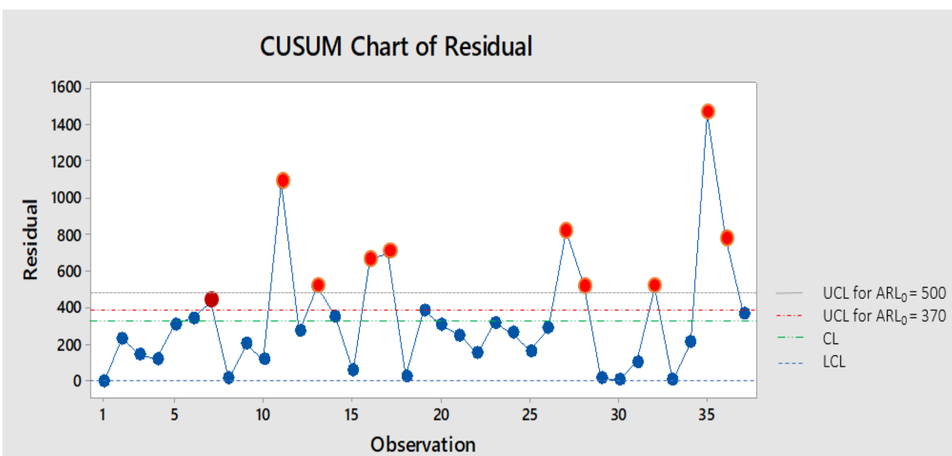

Fig. 1: CUSUM control chart observations with K = 2.5 for the $\text{SARFIMAX}(1,0.0389,1)\times(1,0.4612,1)_{12}$ model fitted to the real dataset.
Source: created by the authors.